Adsorption study of phosphate ions pollution in aqueous solutions using microwave synthesized magnesium oxide nanoparticles

N. A. A. Aboud[a], B. E. Jasim[a], A. M. Rheima[b]
[a]*Department of Chemical Industrial, Institute of Technology/Baghdad, Middle Technical University, Iraq*
[b]*Department of Chemistry, College of Science, University of Waist, Kut, Iraq*

Phosphorus (as phosphate ions) is an essential ingredient that is commonly used in agriculture as both a fertilizer as well as in industry as a detergent which causes significant water pollution. The nanomaterials are mainly involved in removing these ions due to their high surface area. In this study, magnesium oxide nanoparticles (MgO NPs) has been synthesized by microwave method. XRD, AFM and SEM were used to investigate the synthesized MgO nanoparticles. The average particles size of MgO NPs calculated to be range (25-39 nm), and has a cubic structure. The synthesized nanoparticles were tested to remove phosphate ions from aqueous solutions. From the resulted, which found that at a pH 12, temperature 298°C the highest adsorption efficiency of phosphate (72%) as a contact time was 150 minutes. It was found that the adsorption mechanism was spontaneous and endothermic by thermodynamic measurements. Generally, the data indicated a good effectiveness of MgO in the removal of phosphate.

(Received April 10, 2021; Accepted July 6, 2021)

Keywords: MgO NPs, Microwave method, Adsorption, Phosphate ion

1. Introduction

Efficient waste water disposal is a significant requirement for a rising economy in the current age of shortages of water supplies [1-3]. The development and deployment of sophisticated wastewater treatment systems with high performance and low capital requirements is crucial [4-7].

In water sources, nutrient overenrichment (especially nitrogen and phosphorus) has increased eutrophication and facilitated the spread of toxic algal blooms worldwide, which pose a significant threat to the availability of drinking water and the survival of aquatic habitats[8].

Phosphate pollution of surface water is a decline in the suitability of water for human use and affects marine species. Absorption has drawn considerable interest among the potential strategies used to eliminate $(PO_4)^{-3}$ and studies have been performed investigating many new and effective absorbents[9].Among numerous therapies, the interest of scientists has been drawn to recent advanced processes in nano-material sciences[10]. nanotechnology is one of the important technologies in this world [11,12]. It is concerned with the creation, manipulation, and application of nanometer-scale materials [13-16]. It has numerous uses in a variety of sectors, including energy, nanotechnology, and nanobiotechnology [17-21]. nanomaterial has a wide range of applications in different fields like medicine, mechanics, industry, biomedical sciences, environmental health, and engineering [22-25]. In this case scientists discusses the possible advances of nanotechnology with regard to the handling of waste water [26], First, nana-adsorbents[27], like activation carbon[28], carbon nanotubes (CNT) [29], manganese oxide (MnO_2) [30,32], zinc oxide (ZnO) [32], titanium oxide (TiO_2) [33] and iron oxides ($Fe_{(n)}O_{(m)}$), are utilized in the most prevalent application of heavy metals from waste water, have been used as the first class nanomaterials in process wastewater treatment processes[34].

Second, The possibility of removing inorganic and organic pollutants has been shown by nanoscale catalysts like photocatellist, electrocatalyst, fenton-based catalytic and chemical oxidants[35]. Third, nanomembranes are utilized to efficiently eradicate colours, heavy metals and filthy odors by the use of carbon nanotube membranes, electrospun nanofibers and hybrid nano

* Corresponding author: arahema@uowasit.edu.iq

membranes. [36,37]. The aim of this study included preparation MgO NPs by microwave method and To test its effectiveness in removing pollutants from water.

2.1. Synthesis of MgO nanoparticles by Microwave Method

Magnesium oxide nanoparticles was prepared from (1:2 molar ratio) salt to base in aqueous solutions of magnesium nitrate-6-hydrate ($Mg(NO_3)_2.6H_2O$) and Hexamethylenetetramine (HMT) $C_6H_{12}N_4$ [MW= 152.26 $g.mol^{-1}$]. Each of the chemical reagents used were of analytical purity.

Initially, 0.02 mole, 50 ml of HMT was added (drop by drop) to the 0.01 mole, 50 ml of $Mg(NO_3)_2.6H_2O$ using de-ionize water as a solvent and the mixture was stirred for 10 min. then, the solution was transferring to the microwave (SEVERIN-800) for 5 min at 700 Watts. A white turbid precipitate was produced after microwave heating, indicating the forming of $Mg(OH)_2$, Ultrasound treatment was applied for 35 minutes to the product after processing, precipitate centrifuged for 10 minutes then washed many times with de-ionized water and ethanol. The white precipitate was dried in an oven at 85 ℃ for 1 hours then calcination in furnace at 700 ℃ for 4 h which gave a white precipitate has been collected from MgO NPs

2.2. Preparation of Phosphate solution

Dissolved (0.439g) in deionized water of potassium dihydrogen phosphate (KH2PO4) for preparation of a stock solution of phosphate ion with a starting concentration of 1000 mg/l, required to work solutions were generated by additionally diluting a stock solution of deionized water for the different concentrations between 50 to 250 ppm phosphate at the required initial concentratation.. Recipe and Preparation of pH (2.0-6.0) buffer by 0.2 M of Hydrochloric Acid (HCl) and 0.2M of Potassium Chloride (KCl) . the 0.1M of sodium carbonate (Na_2CO_3) and 0.1M of sodium bicarbonate ($NaHCO_3$) reagent used to hold pH (8.0-12.0) samples is the bicarbonate buffer solution.

3. Results and discussion

3.1. X-ray diffraction (XRD)

The X-ray diffraction technique with an X-ray wavelength of Cu Ka radiation at a scanning rate of 2 theta from 10˚- 80˚. The diffraction peaks of 2θ = 36.49˚, 42.64˚ and 62.14˚ were recorded in the XRD pattern relating to diffraction phases (111), (200) and (220) respectively as can seen in figure (1). The phase detection was conducted and can be indexed to cubic MgO planes (JCPDS 43-1022), the average crystalline size (D) of a synthetic MgO NPs was calculated by Scherer's equation [15,16].

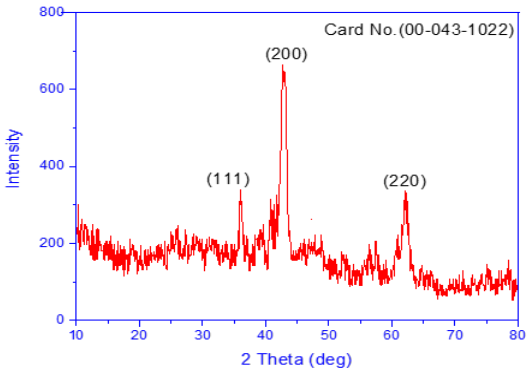

Fig. 1. XRD pattern of MgO NPs.

3.2. Atomic force microscopy (AFM)

The atomic force microscopy (AFM) was using to investigate the morphology of nano-synthesized surfaces by (model AA3000, Angstrom Advanced Inc., USA). Figure (2a) illustrate 3D image of nanoparticles, MgO NPs has a hemispherical shape vertically comparable grains with homogeneity of the surface while figure (2b) illustrate the Granularity accumulation distribution chart Diameter (<=90% :39.00 nm),(<=50%: 34.00 nm) and (<=10%: 22.00 nm), with average grain size diameter:33.67 nm.

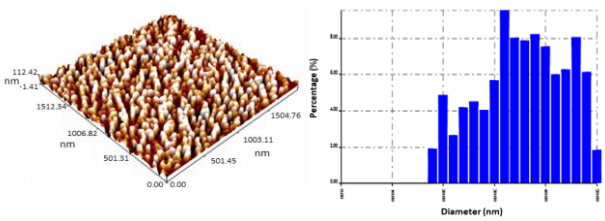

(a) 3D image

(b) Granularity accumulation

Fig. 2. AFM of MgO.

3.3. Field emission scanning electron microscope (FE-SEM)

The Figure 3 reveals morphology of magnesium oxide nanoparticles that are demonstrates the crystalline existence of MgO NPs having particles size approximately ~25 nm which is complying with average crystallite size (D) obtained by XRD using Scherrer's equation. Where through an image we notice a smooth surface and the presence of high pores on the surface and that the particles do not contain any clumps.

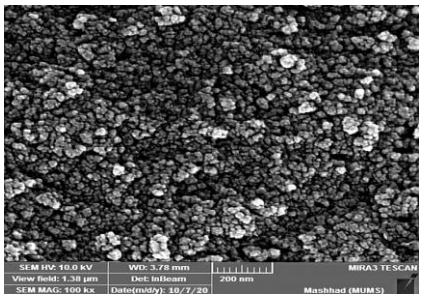

Fig. 3. FE-SEM MgO nanoparticles.

3.4. Adsorption study

3.4.1. Determine the time required for equilibrium

To finding the contact time between the adsorbate and adsorbent at equilibrium, the appropriate concentration of phosphate ion was determined and placed in contact with 0.01 gm of MgO and 50 ml of 100 ppm of phosphate ion at 25℃ in the shaker, in successive periods of time and analyzed. To find out the change in concentration with the passage of time, the time required for equilibrium to occur was 150 minutes, the reason for the high equilibrium time is due to the nanomaterial prepared for binding to the phosphate ion.

3.5. Effect of Temperature

The temperature effect on the adsorption of $(PO_4)^{-3}$ was studied at (25,35,45,55) ℃ and it was found that the amount of adsorption increases with increasing temperature as see in figure (4),

meaning that the process is of the endothermic type (physical adsorption) . The reason for this may be attributed to the fact that the adsorption is accompanied by an absorption process [38,39] , whereby the adsorbed particles diffuse into the pores and the crystal network of the nanomaterial and the speed of their diffusion increases with increasing temperature. Such behavior is attributed to the occurrence of the sorption process and this is an endothermic process.

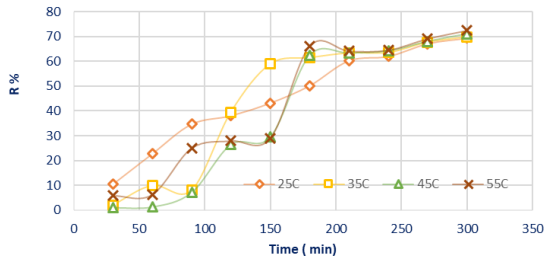

Fig. 4. Effect of time on the Adsorption of phosphate ions by different temperatures.

3.6. Effect of PH

The acidic function of phosphate ion removal was studied by using 0.01 gm of MgO NPs and 50 ml of 200 ppm of phosphate ion at a pH ranging between (2-12). The pH value affects the effective adsorption sites on the adsorption surface as for the basic medium, the adsorption rate increases on the surfaces of the adsorption materials, and the best results for adsorption are achieved in the basic media, the figure (5) domonstrates effect of the acidic function on the percentage of $(PO_4)^{-3}$ adsorption [40,41] .

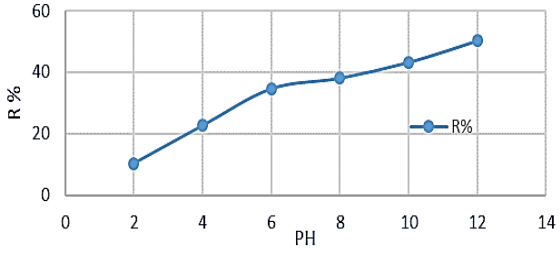

Fig. 5. Effect of PH on the Adsorption of phosphate ions.

3.7. Adsorption isothermal

In this study two types of isotherms were used, Figure (6) illustrates Langmuir and Freundlich isothermal models will model with experimental data for phosphate ion $(PO_4)^{-3}$ adsorption from their solution [42-43] .Equation (2) gives the Langmuir isotherm

$$\frac{C_e}{Q_e} = \frac{1}{a} + \frac{b}{a} C_e \quad (1)$$

where a and b represent the Langmuir constants , C_e is $(PO_4)^{-3}$ concentration at equilibrium while Qe describes the quantity of adsorption corresponding to monolayer adsorption. In the solutions, the Langmuir equation was used to calculate the adsorption curves of (P), as can be seen in relation between (C_e) versus (C_e/Qe) in Figure (A).
The Freundlich equation[44]

$$\log (Q_e) = \log(k_f) + \left(\frac{1}{n}\right) log (C_e) \quad (2)$$

where k_f and n showed the Freundlich constants, which are the adsorption capacity and the adsorption intensity. On heterogeneous surfaces for adsorption, the Freundlich equation was developed and the adsorption curves of $(PO_4)^{-3}$ were modified to a Freundlich equation as shown in the relationship between (ln Q_e) versus (ln C_e). According to the data results (A and B), $(PO_4)^{-3}$ adsorbs using the Freundlich equation, which is suitable for surface multilayer adsorption.

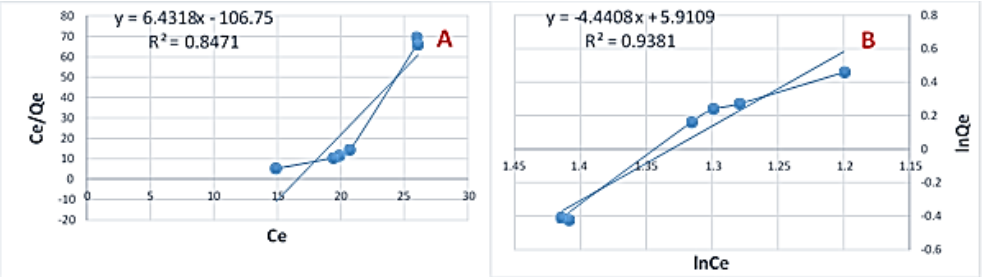

Fig. 6. Adsorption curves of (A) as Langmuir isotherm, (B) Freundlich isothermal at 298 K.

3.8. Thermodynamic study

An adsorption process thermodynamic analysis was done in this study. The effect of temperature on phosphate adsorption was studied use nano-adsorbent MgO synthesized in the range of 25–55°C as show in Fig.7.

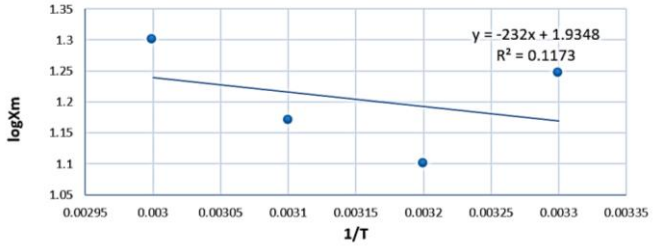

Fig. 7. The relation between log X_e and 1/T for the adsorption of $(PO4)^{-3}$.

The (ΔG), (ΔH) and (ΔS) of adsorption were estimated using equations (4 , 5) to anticipate the process of adsorption.

$$\log x_m = \frac{-\Delta H}{2.303R} + \frac{\Delta S}{R} \tag{3}$$

$$\Delta G = \Delta H - T\Delta S \tag{4}$$

where x_m is the maximum adsorbate concentration (mg/g), R is the gas constant (8.314 J/mol ∗ K) and T is the temperature (K). As seen in Figure(8) ΔH was calculated from the slope of the van't Hoff plots of log (x_m) versus (1/T) and (ΔS) was calculated from the (y axsis) intercept . the value of ΔH form slope was 4.4 KJ\mole , which indicated the adsorption was endothermic. The ΔS from intercept was 19.08 J(mol*K) that indicated The adsorbed particles are in constant motion on the surface. The ΔG was – 1.8 KJ\mole at 328 K , which mean the adsorption is spontaneous [45,46].

4. Conclusion

In this study, Phoshate ions remove from aqueous solutions using magnisum oxide nanoparticles, MgO NPs prepared with average crystallite size (15.38) nm from XRD , grain size (33.67) nm from AFM and (25) nm from SEM . To that end, the influence of different parameters is analyzed (as different pH, contact time and temperature) were studied. The experiments have shown that pH = 12 was the perfect conditions to remove the phosphate ion the highest rate of phosphate ion adsorption was estimated to be 72%. Langmuir and Freundlich isotherm models were used to analyze the equilibrium activity of the $(PO_4)^{-3}$ ion removal process.The results revealed that Freundlich isotherm models would reliably characterize the adsorption process' equilibrium behavior. Thermodynamic parameters for Phoshate ion adsorption mechanism were also obtained, adsorption mechanism was found to be attractive physical, endothermic and spontaneous.

References

[1] P. Kehrein, M. Van Loosdrecht, P. Osseweijer, M. Garfí, J. Dewulf, J. Posada, Environ. Sci. Water Res. Technol. **6**(4), 877 (2020).
[2] E. T. Sayed, N. Shehata, M. A. Abdelkareem, Sci. Total Environ. **748**, 141046 (2020).
[3] Á. Robles, D. Aguado, R. Barat, Bioresour. Technol. **300**, 122673 (2020).
[4] P. Biniaz, N. T. Ardekani, M. A. Makarem, M. R. Rahimpour, Chem. Engineering **3**(1), 1 (2019).
[5] H. Yi, M. Li, X. Huo, Crit. Rev. Biotechnol. **40**(1), 99 (2020).
[6] A. Ullah, S. Hussain, A. Wasim, M. Jahanzaib, Sci. Total Environ. **731**, 139158 (2020).
[7] A. AlSayed, M. Soliman, A. Eldyasti, Renew. Sustain. Energy Rev. **134**, 110367 (2020).
[8] B. Wu, J. Wan, Y. Zhang, Environ. Sci. Technol. **54**, 50 (2020).
[9] S. Mazloomi, M. Yousefi, H. Nourmoradi, J. Environ. Heal. Sci. Eng. **17**(1), 209 (2019).
[10] I. Bavasso, G. Vilardi, M. Stoller, Chem. Eng. Trans. **47**, 55 (2016).
[11] A. H. Ismail, H. K. Al-Bairmani, Z. S. Abbas, A. M. Rheima. IOP Conf. Ser.: Mater. Sci. Eng.928 052028 (2020).
[12] A. H. Ismail, H. K. Al-Bairmani, Z. S. Abbas, A. M. Rheima.. Egyptian journal of chemistry; 63 (7) 1 2020
[13] A. H. Ismail, H. K. Al-Bairmani, Z. S. Abbas, A. M. Rheima, Nano Biomed. Eng. 12(2), 139 (2020)
[14] AT Salman, AH Ismail, AM Rheima, AN Abd, NF Habubi, ZS Abbas. In Journal of Physics: Conference Series 2021 Mar 1 (Vol. 1853, No. 1, p. 012021). IOP Publishing
[15] A. M. Rheima, A. A. Anber, H. I. Abdullah, A. H. Ismail, Nano Biomed. Eng. **13**(1), 1 (2021).
[16] A. M. Rheima, M. A. Mohammed, S. H. Jaber, S. A. Hameed, Journal of Southwest Jiaotong University **54**(5), 2019.
[17] A. M. Rheima, M. A. Mohammed, S. H. Jaber, M. H. Hasan, Drug Invention Today 12(11), 2818 (2019)
[18] A. H. Ismail, H. K. Al-Bairmani, Z. S. Abbas, A. M. Rheima. Nano Biomed. Eng;12(3):253 (2020)
[19] A. Rheima, A. A. Anber, A. Shakir, A. Salah Hammed, S. Hameed, Iranian Journal of Physics Research **20**(3), 51 (2020).
[20] A. F. Kamil, H. I. Abdullaha, A. M. Rheima, W. M. Khamisa,2021. (Vol. 17, No. 3, May June 2021, P.). Journal of Ovonic Research.
[21] A. M. Rheima, D. H. Hussain, H. J. Abed, In IOP Conference Series: Materials Science and Engineering **928**(5), 052036 (2020). IOP Publishing.
[22] A. M. Rheima, D. H. Hussain, M. M. Almijbilee, Journal of Southwest Jiaotong University **54**(6), 2019.
[23] SN Aziz, MF Al Marjani, AM Rheima, IM Al Kadmy. Reviews in Medical Microbiology.

2021 Apr 9
[24] A. M. Rheima, N. A. Aboud, B. E. Jasim, A. H. Ismail, Z. S. Abbas, International journal of pharmaceutical research **13**(1), 2021.
[25] H. A. Kadhum, W. M. Salih, A. M. Rheima, Applied Physics A **126**(10), 1 (2020).
[26] M. Hull, D. Bowman, Nanotechnology environmental health and safety: risks, regulation, and management. William Andrew, 2018.
[27] M. Anjum, R. Miandad, M. Waqas, F. Gehany, M. A. Barakat, Arab. J. Chem. **12**(8), 4897 (2019).
[28] L. S. Rocha, D. Pereira, É. Sousa, Sci. Total Environ. **718**, 2020.
[29] R. Das, S. B. Abd Hamid, M. E. Ali, A. F. Ismail, M. S. M. Annuar, S. Ramakrishna, Desalination **354**, 160 (2014).
[30] H. Esmaeili, R. Foroutan, D. Jafari, M. Aghil Rezaei, Korean J. Chem. Eng. **37**(5), 804 (2020).
[31] W. Lan, J. Zhang, Z. Hu, Chem. Eng. J. **335**, 209 (2018).
[32] B. Jain, A. Hashmi, S. Sanwaria, Adv. Compos. Hybrid Mater. **3**(2), 231 (2020).
[33] P. Delaney, C. McManamon, J. P. Hanrahan, J. Hazard. Mater. **185**(1), 382 (2011).
[34] J. Yang, B. Hou, J. Wang, Nanomaterials **9**(3), 2 (2019).
[35] M. Nasrollahzadeh, M. Sajjadi, S. Iravani, Carbohydr. Polym. **251**, 116986 (2021).
[36] O. Agboola, P. Popoola, R. Sadiku, in Environmental Nanotechnology **3**, 1 (2020).
[37] M. Kamali, K. M. Persson, Environ. Int. **125**, 261 (2019).
[38] H. Zhang, J. Hu, J. Xie, RSC Adv. **9**(4), 2011 (2019).
[39] A. M. Rheima, R.S Mahmood, D.H. Hussain, Z.S. Abbas, Digest Journal of Nanomaterials and Biostructures; **16(**1), p.11-18, (2021)
[40] J. Aravind Kumar, D. Joshua Amarnath, S. Anuradha Jabasingh, J. Clean. Prod. **237**, 117691 (2019).
[41] N. A.A. Aboud , B. E. Jasim , A. M. Rheima, Chalcogenide Letters , Vol. 18, No. 5, May 2021, p. 237 – 243.
[42] M. A. Mohammed, A. M. Rheima, S. H. Jaber, S. A. Hameed, Egyptian Journal of Chemistry **63**(2), 5 (2020).
[43] D. H. Hussain, A. M. Rheima, S. H. Jaber, M. M. Kadhim, Egyptian Journal of Chemistry **63**(2), 417 (2020).
[44] A. M. Rheima, M. A. Mohammed, S. H. Jaber, S. A. Hameed, Desalination and Water Treatment **194**, 187 (2020).
[45] A. F. Kamil, , H. I.Abdullah, A. M. Rheima, S. H. Mohammed, *Egyptian Journal of Chemistry* (2021).